23rd Australasian Fluid Mechanics Conference - 23AFMC
Sydney, Australia
4 – 8 December 2022
Paper No: AFMC2022-097

A Practical Numerical Approach to Predict the Skin Friction Drag on a Rough Surface

Setyo Nugroho [1*], Eric Fusil [1], Bagus Nugroho [2], and Rey Chin [1]

[1]School of Mechanical Engineering, The University of Adelaide, Adelaide, SA, 5005, Australia
[2] Department of Mechanical Engineering, The University of Melbourne, Melbourne, VIC, 3010, Australia
*mailto: setyo.nugroho@adelaide.edu.au

Abstract

A steady Reynolds Averaged Navier-Stokes simulation scheme is performed to study the friction characteristics in the turbulent boundary layer on various rough surfaces. Comparisons of the characteristics, including the skin friction drag, are analysed to examine the variation between the irregular rough surface and the equivalent sand grain roughness model. The irregular rough surfaces are modeled by randomly distributed hemispheres with a 1 mm height, covering 5%, 10%, 20%, and 30% of a flat plate's area, and designed to represent the three-dimensional roughness. The roughness dimension and the area coverage correlate with a roughness parameter called the roughness density factor to determine the equivalent sandgrain roughness value. This work aims to find a relationship between the irregular roughness and the equivalent sand grain roughness, based on a similarity of friction characteristics, and to give practical guidance about flow simulations over a rough surface. The relationship between these elements suggests an approach to determining equivalent sand grain roughness that can be applied to the computational fluid dynamics solver. The equivalent sand grain roughness model enables the prediction of the skin friction drag using a simple numerical simulation procedures and significantly reduces the computational cost with acceptable accuracy. The results suggest there is a simple correlation with a correction factor between the irregular roughness and equivalent sand grain roughness.

1 Introduction

The relationship between roughness and skin friction drag had been investigated extensively in the last six or seven decades, either experimentally or numerically. Indeed, both approaches need abundant resources, for instance, an experiment approach needs a towing tank or wind tunnel to measure the drag and flow characteristics. In addition, the numerical approach using computational fluid dynamics (CFD) method needs hours of simulation time and a high-performance computer with parallel processing.

This paper discusses about turbulent boundary layer (TBL) over various coverage areas of roughness surfaces to develop a deep understanding of the relationship between the skin friction drag and the coverage area of the roughness on a surface. To study the relationship, first, the natural roughness, which occurs three-dimensionally, was modelled with uniform size hemispheres with various area coverages over a surface. The hemispheres are considered the simplest form of a three-dimensional roughness model because their surface can be easily modeled by a simple function, and the coverage area will represent the progression of biofouling growth on a surface. The hemispheres then will be distributed randomly on the model to mimic natural roughness.

The natural roughness model was then simulated using the CFD method to understand the flow characteristics near the wall. Our work used commercial CFD software ANSYS-Fluent, which is

more practical to use in industry. This paper aims to provide practical guidelines to correlate the natural roughened surface with particular areas of coverage to the build-in equivalent sand-grain roughness model, which is commonly used, and calculate skin friction drag with simpler procedure and lower computational cost.

Surface roughness increases turbulent stress and wall shear stress. On a rough surface, the log-law mean velocity profile is given by

$$U^+ = \frac{1}{\kappa}\ln y^+ + B - \triangle U^+. \tag{1}$$

where U^+ is the non-dimensional velocity in the boundary layer and y^+ is the non-dimensional normal distance from the boundary. These terms are further defined as follows $U^+ = \frac{U}{U_\tau}$ and $y^+ = \frac{U_\tau y}{\nu}$, where U is the mean velocity, U_τ is the friction velocity defined as $\sqrt{\frac{\tau_w}{\rho}}$, y is the normal distance from the wall, ν is the kinematic viscosity, τ_w is the shear stress magnitude, and ρ is the density of the fluid. Note that $\triangle U^+ \equiv 0$ for a smooth wall. It should also be noted that the shift in velocity profile is manifested as an increase in frictional resistance owing to momentum loss. The value of $\triangle U^+$ is typically obtained experimentally, since there is no universal roughness function model for every kind of roughness.

Even though roughness may be characterised using various ways, the roughness height, k, and equivalent sandgrain roughness height, k_s are the keys to define how rough the surface is. The roughness Reynolds number k_s^+ explains the critical parameter depicting roughness effects on the flow near the surface. The roughness height can be normalised and termed the roughness Reynolds number, given by $k_s^+ = \frac{k_s U_\tau}{\nu}$.

When k_s^+ is low, e.g. less than 5 as in Nikuradse's sandgrain roughness, wall roughness does not affect the viscous sublayer region; the viscous sublayer is intact and undisturbed Nikuradse (1933). This condition is termed as a hydraulically smooth regime. Along with the increment of k_s^+, the regime turns into a transitionally rough regime. In this regime, fluid viscosity cannot absorb the turbulent eddies produced by the roughness and create Reynolds stress, along with the viscous stress, which contributes into the total skin friction. With the increase of k_s^+, the roughness function obtains a linear asymptotic. This region at high k_s^+ is the region termed a fully rough regime. In a fully rough regime, the skin friction drag coefficient is unaffected by the Reynolds number, and the drag on the roughness surface is the prominent factor responsible for the momentum deficit.

Researchers have been developing correlations for the roughness function that span from basic models based on roughness height to the more complex connections involving density and form parameters. Waigh & Kind (1998) reported further three-dimensional roughness prediction correlations. Their correlations were based on the outcomes of roughness element forms such as flat plates, blocks, cubes, rods, cylinders, spheres, cones, and hemispheres. They modified Simpson's density parameter Simpson (1973) with the streamwise aspect ratio (ratio of the roughness height to the roughness length), and they highlighted how the correlations for roughness shapes were achieved in regular patterns, emphasising the necessity of discovering methods for parameterising the geometry of natural roughness. Sigal & Darnberg (1990) investigated the influence of roughness density in a new way, incorporating the reference surface area before roughness addition and the overall roughness frontal area. van Rij *et al.* (2002) extended the use of this measure to three-dimensional regular roughness by introducing the total windward wetted surface area to calculate the roughness density factor parameter, λ. We correlated the roughness density factor parameter to the equivalent sand-grain roughness by the method that described by van Rij *et al.* (2002). The result of the correlation is shown in Table 2.

2 Numerical scheme

CFD simulations have recently gained a considerable amount of interest and have become an important tool for studying the effect of roughness on a surface. Three-dimensional fluid flow across a flat plate will be observed to determine the flow characteristics, the viscous drag, and the boundary layer's thickness. The CFD model was developed based on the steady Reynolds Averaged Navier-Stokes (RANS) equation using a commercial CFD software package ANSYS-Fluent. The momentum equations were solved using the second-order upwind convection technique. The simulation was built on a Semi-Implicit Method for Pressure-Linked Equations (SIMPLE) method. The shear stress transport (SST) k − ω turbulence model was applied to simulate the near-wall flow, which hybrid the benefits of the k − ω and the k − ε turbulence model Menter (1994).

There are two simulation cases to investigate the relationship between the random roughness with a specific area coverage and the sandgrain roughness model. The cases (i) are randomly distributed hemispheres and (ii) flat plate with sandgrain roughness entirely. These cases use double-body simulation, which treat the upper boundary as a symmetry boundary condition in order to mitigate the wave-making behaviour and hence there is only viscous force involved Song *et al.* (2020). An illustration of the computational domain can be seen in Fig. 1. The inlet is set as a velocity inlet with 10 m/s velocity with L = 2000.

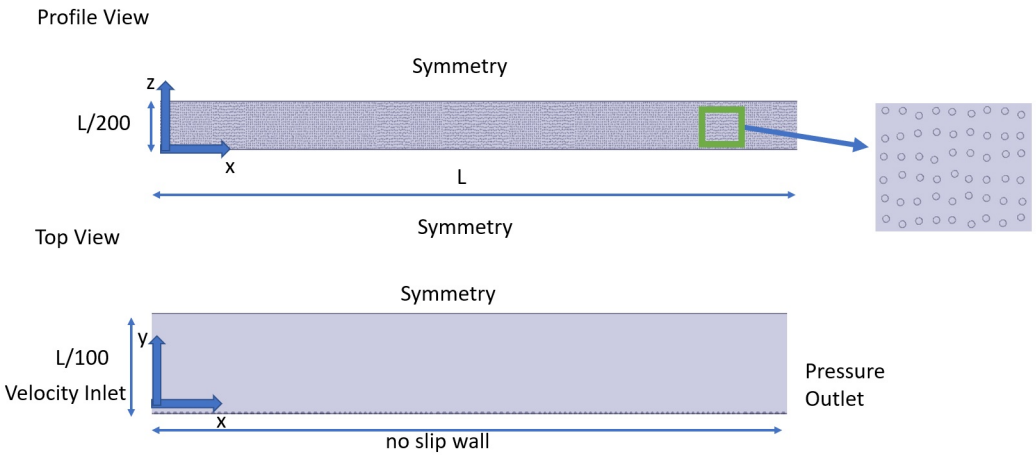

Figure 1. Computational domain for case (i) CFD simulation with inset describe randomly distributed roughness with no overlapping

The roughness was modelled by hemispheres with 2 mm diameters, which are considered as a representative size of the natural roughness size on a ship, that cover 5%, 10%, 20%, and 30% of the area coverage. An algorithm was developed to generate randomly distributed hemispheres. The distribution is set up without overlap between the hemispheres by using built in random function in Matlab software. The random function was applied to place the center of the hemispheres in a small grid area to prevent overlap. the The randomly distributed hemispheres roughness is described in inset of Fig.1.

The mesh near the random hemisphere simulation used unstructured tetrahedral mesh generated using the built-in meshing tool of ANSYS Meshing. The mesh was generated to resolve the velocity profile in the inner sub-layer of the boundary layer. The mesh first layer mesh was set to obtain $y^+ < 1$. There are 25 layers of mesh to analyse the boundary layer. This simulation used over 80 million tetrahedral cells with acceptable mesh quality. On the other hand, the sand-grain roughness simulation applied the structured hexagonal mesh on the walls that was generated with the same parameters.

Inaccuracies in determining the y value of the data point closest to the wall might cause an unfit curvature in the log-law area of the mean velocity profile. In general, measurements in normal direc-

tion of a surface are started from a shifting in arbitrary zero plane origin ε. This ε value is used to induce a linear log-law, and Perry *et al.* (1969) propose a straightforward approach for determining ε. Firstly, a plot of U/U_e vs. log y is created, where U_e is the free-stream velocity. In the log-law area, the plot should fit a linear or slightly curved trend. A faired curve is drawn through the log-law region. If the faired curve is concave up (positive second derivative), a positive ε is added to each y data point, and the curve is re-plotted. If the faired curve is concave down (negative second derivative), a negative ε is applied to all y data points, and the curve is re-plotted. This method is iterated until linearity is achieved in the log-law region.

Referring to the Townsend wall similarity Townsend (1980), in the beneath of viscous sub-layer, turbulent motions are unaffected by surface characteristics and viscosity when the Reynolds number is high. This similarity suggests that the turbulent stress, normalised by the wall shear stress, is universal outside of the roughness sub-layer. According to the research conducted by Raupach *et al.* (2015) and Jimenez (2013), the outside section has been widely assumed to be independent of the roughness. This means that in the overlap and outer region of the boundary layer, the mean velocity profile for both smooth and rough walls obey the universal velocity defect law. Therefore, friction velocity could be determined that make a good collapse of mean velocity profiles in the outer region. After the friction velocity was determined, the wall shear stress and skin friction drag coefficient can be calculated as $c_f = \frac{2\tau_w}{\rho U_e^2}$.

Since the drag increment is the primary concern in engineering applications, the main objective of the simulation is to obtain the mean velocity profile. After the mean velocity profile acquired, the ε was determined using Perry's procedure Perry *et al.* (1969) as explained. The ε value itself should be between zero and the maximum roughness height. However, the ε should give a good collapse between outer region mean velocity profile and velocity defect law. Therefore, ε = 100 μm was selected to all of the surfaces.

The selected ε is then accounted to calculate the velocity defect law. To determine the friction velocity, Townsend's similarity law was applied at the $x/L = 0.75$, where this location was considered in a fully rough condition. The value U_τ was set to give the best fit of the velocity defect law using the polynomial equation described by Djenidi *et al.* (2019).

This procedure is then applied to specific streamwise positions to obtain the U_τ along the wall in the streamwise direction. The determined friction velocity then was used to calculate the skin friction coefficient along the surface. Afterwards, the comparison of cases (i) and (ii) will be made to find the corresponding value of the sandgrain height roughness model. A smooth wall simulation using DNS was used to check the validity of the CFD results obtained in this work. From these CFD results, correlating values and correction factor are expected to be found, and some of the limitations of these simulations can be determined.

3 Results and discussion

3.1 Mean Velocity Profile

The mean velocity profile is a key parameter to determine the flow characteristics on a surface. The summary of flow characteristics on both cases can be seen in Table 1. These results show a similarity between both cases, e.g 5%, 10%, 20%, and 30% area coverage are similar to k_s 125 μm, k_s 250 μm, k_s 500 μm, and k_s 750 μm respectively. The results also show the coverage area only contributes less than 20% of the boundary layer thickness growth. Fig.2(a) describes the effect of coverage area of the roughness to the mean velocity profile on position $x/L = 0.75$. The plot shows that there is a downward shift in mean velocity profile due the increase of coverage area of the roughness. Fig.2(b) shows the collapse of velocity defect at the outer region. This collapse indicates that the flow obeys Townsend's similarity law on the outer region.

Table 1. Summary of CFD Results at x/L = 0.75

Surface	U_τ (m/s)	δ (mm)	Re_τ	C_f
Smooth	0.037	0.12	2025	0.002
5% area coverage	0.4317	24.7	8391	0.0035
10% area coverage	0.4837	26.4	10027	0.0044
20% area coverage	0.5198	28.8	11769	0.0050
30% area coverage	0.5373	28.2	11891	0.0053
k_s = 125 μm	0.439	22	7603	0.0039
k_s = 250 μm	0.4776	27	10129	0.0046
k_s = 500 μm	0.5139	31.9	12894	0.0053
k_s = 750 μm	0.5371	36.9	15564	0.0058

The rough wall streamwise mean velocity profile is compared with a smooth wall DNS results Chan *et al.* (2021) to observe their slope matching in the log-law region. This mean velocity profile agrees with Schultz *et al.* (2015) which mentions that the ΔU^+ is a function of k_s^+, This roughness function has the best agreement with the roughness function model (equation 1) obtained by Marusic *et al.* (2013) with $\kappa = 0.39$ and $B = 4.3$.

Then, the mean velocity profile will be used to obtain a downward shift of U^+ to determine the roughness function and the correlated sandgrain roughness. This shift is correlated with a momentum deficit that leads to higher skin friction drag, which is consistent with the data in Table 1. The roughness function is shown in Fig.3 that shows the roughness function ΔU^+ as a function of the equivalent sand grain roughness k_s^+ in a fully rough regime. Generally, the CFD results can collapse well to the fully rough asymptotic line, which suggests that the flow considered in the fully rough regime indicated in high k_s^+ values. Furthermore, Fig.3 shows that there is no collapse of roughness function in upstream region. This is an indication that in upstream region, the flow regime might not be considered as fully rough condition.

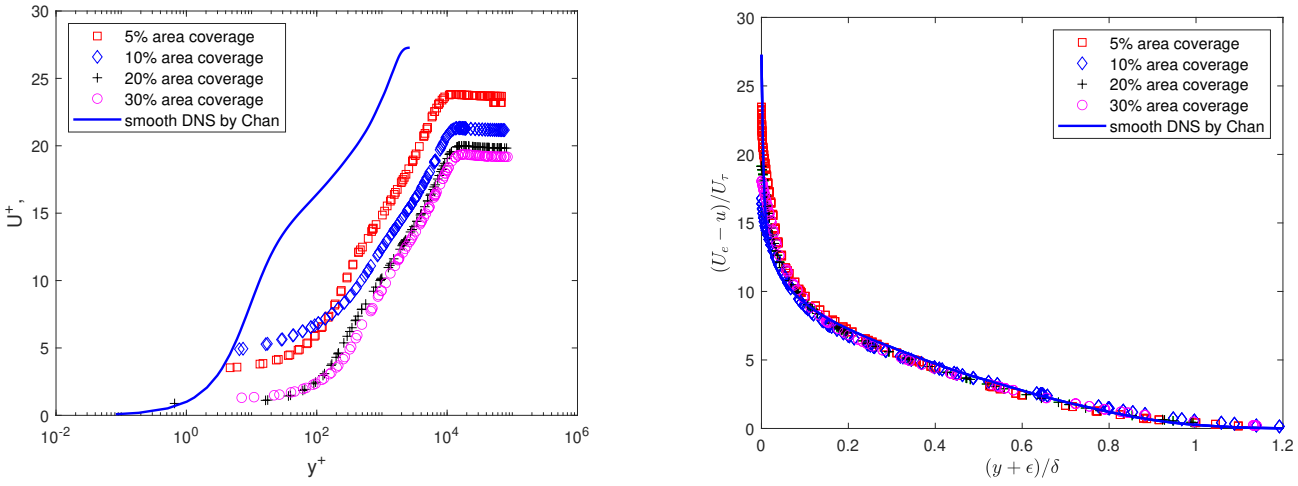

(a) (b)

Figure 2. (a) The streamwise mean velocity profile at x/L = 0.75 (b) Velocity defect profile at x/L = 0.75

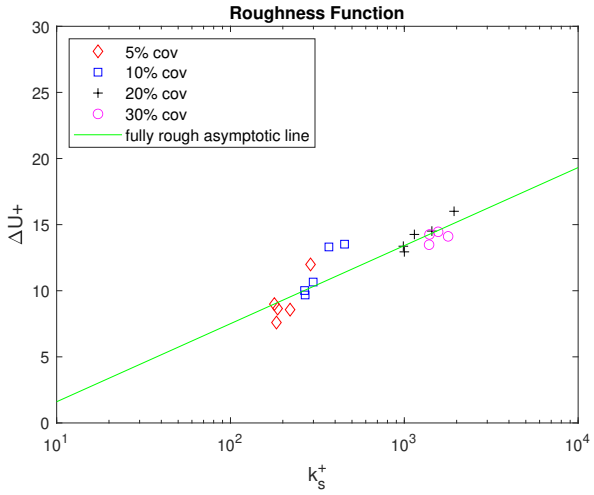

Figure 3. Roughness function as a function of equivalent sand grain roughness height normalised by the inner length compared with a fully rough asymptotic line

3.2 Skin Friction Drag Increment

The predicted k_s^+ from roughness function was then used to calculate k_s and compared to the CFD case (ii) simulation with a particular value of sandgrain roughness model on a flat plate. A correction factor was determined to give a more accurate relationship between the area coverage and sandrgrain roughness model. The summary can be seen in Table 2. This result is comparable with an experiment using close-packed spheres performed by Schultz Schultz & Flack (2005) which states that the difference between actual and predicted k_s is about 30.8% Flack & Schultz (2010).

A mean velocity profile in $x/L = 0.75$ is plotted in Fig.4(a). This $x/L = 0.75$ position is considered in a fully rough region due to the constant wall shear stress. For instance, Fig.4(a) shows that the mean velocity profile of 10% area coverage of case (i) results have a good similarity of to the mean velocity profile of closed pack sandgrain roughness with the height of 250 μm. The other data are not shown due to clarity reason. The plot has a good collapse in the outer region, which indicates a match in Reynolds number between case (i) and case (ii). This collapse is consistent with Townsend's outer layer similarity, suggesting that the turbulent flow is independent of viscous shear stress in high Reynolds number. However, in the inner layer, there is a difference in the mean velocity profile between case (i) and (ii) due to a difference in ε employed. The sandgrain model, which ANSYS-Fluent runs, uses the default setting of the software: a half of the sandgrain roughness model height.

Fig.4(b) shows that in some Reynolds number values, the friction velocity remains constant and leads to a constant skin friction drag. Fig.4(b) also suggests that there is a good match between the skin friction drag coefficient in case (i) and case (ii), and the flow becomes a fully rough regime in x/L less than 0.5 regardless of the area coverage of the roughness. These results suggest that procedure in case (ii) can be applied to predict the mean velocity profile and skin friction drag in natural roughness conditions with a certain coverage areas.

The skin friction drag coefficient from both cases were then compared with the smooth flat plate's friction drag coefficient to determine the skin friction drag increment. The depiction of the comparison can be seen in Fig.5. This current result agrees with the reference value that stated the drag coefficient for a flat plate in turbulence flow is around 0.002. There is a about 180% increment in C_f compared with the smooth wall due to 30% area coverage.

To correlate the case (i) roughness parameter with the equivalent sandgrain roughness, a different approach to predict k_s was performed by using λ parameter described by van Rij *et al.* (2002). The comparison of the relationship between the sandgrain roughness height determined from cases (i), (ii), and λ are listed in Table 2. From case (ii) results, it can be seen that the triple coverage area corresponds with the triple equivalent sandgrain roughness height. In addition, the equivalent sandgrain

Table 2. Comparison of k_s for each area coverage of roughness

Area Coverage	5%	10%	20%	30%
λ	121.37	60.68	30.30	20.10
Predicted k_s (μm) by λ	225	594	1300	1700
Predicted k_s (μm) case i	690	820	2990	3820
Predicted k_s (μm) case ii	125	250	500	750
Constant factor	0.55	0.42	0.38	0.42

roughness height of case (ii) can be predicted by multiply equivalent sand-grain roughness height calculated from λ with some constant factors. For instance, to predict k_s value as ANSYS-Fluent input for 10% area coverage of roughness, a constant factor of 0.42 can be used. Therefore, the prediction of equivalent sandgrain roughness height can be calculated by using λ of the rough surface. There is an indication of the linear relationship between the coverage area of the roughness and the equivalent sandgrain roughness model. However, this relation needs to be examined on the higher area coverage of roughness to determine its limitation.

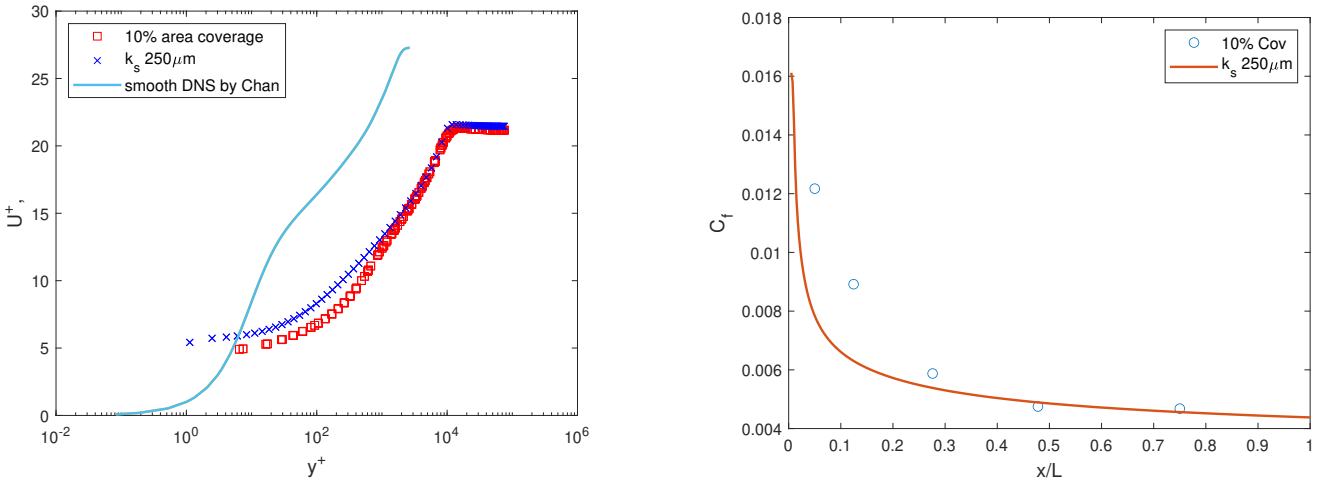

(a) (b)

Figure 4. Comparison of case (i) and case (ii) (a) mean velocity profile at the fully rough region $x/L = 0.75$ 10% area coverage (b) skin friction drag coefficient along the surface

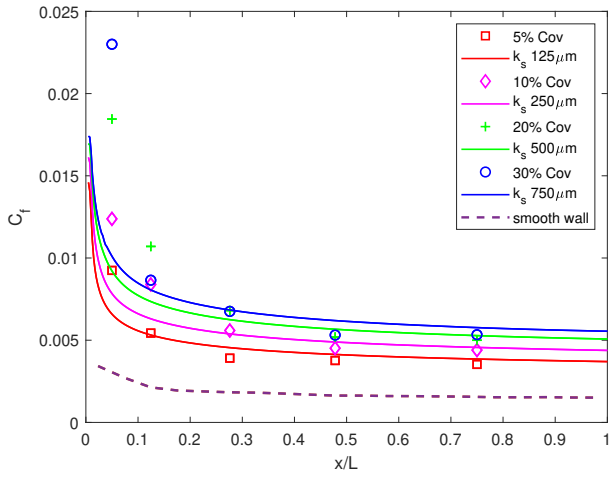

Figure 5. Skin friction coefficient comparison between smooth wall, 5%, 10%, 20%, and 30% area coverage of roughness

4 Conclusions

It can be concluded that there is a linear correlation between randomly distributed hemispheres roughness with a specific area coverage and the sandgrain roughness model provided by the well-known commercial CFD software ANSYS-Fluent. The relationship gives a reasonable accuracy for the skin friction drag coefficient prediction, which is beneficial in naval engineering. The skin friction drag of a fouled ship can be predicted by the sandgrain roughness model with some correction factor that is relatively straightforward with a low computational cost and suitable for engineering applications. However, there is a constrain in the algorithm of ANSYS-Fluent regarding its ε value in the sandgrain roughness model. ANSYS-Fluent uses close packed sandgrain roughness with a certain height k_s, and it automatically sets the ε as $k_s/2$. This value might be contributing to uncertainty, especially in the inner region boundary layer. In addition, the relation should be further examined to be applied in higher area coverage.

References

Chan, C.I., Schlatter, P., and Chin, R.C. 2021, Interscale transport mechanisms in turbulent boundary layers, Journal of Fluid Mechanics, vol. 921.

Djenidi, L., Talluru, K., and Antonia, R. 2019, A velocity defect chart method for estimating the friction velocity in turbulent boundary layers, Fluid Dynamics Research, vol. 51, no. 4, p. 045502.

Flack, K.A. and Schultz, M.P. 2010, Review of hydraulic roughness scales in the fully rough regime, Journal of Fluids Engineering, Transactions of the ASME, vol. 132, no. 4, pp. 0 412 031–04 120 310.

Jimenez, J. 2013 Near-wall turbulence, Physics of Fluids, vol. 25, no. 10.

Marusic, I., Monty, J.P., and Hultmark, M. 2013, On the logarithmic region in wall turbulence, Journal of Fluid Mechanics, no. September 2014.

Menter, F.R. 1994, Two-equation eddy-viscosity turbulence models for engineering applications, AIAA Journal, vol. 32, no. 8, pp. 1598–1605.

Nikuradse, J. 1933, Laws of flow in rough pipes, NASA Tech. Memo. 1292.

Perry, A.E., Schofield, W.H., and Joubert, P.N. 1969, Rough wall turbulent boundary layers, Journal of Fluid Mechanics, vol. 37, no. 2, pp. 383–413.

Raupach, M.R., Antonia, R.A., and Rajagopalan, S. 2015, Rough-wall turbulent boundary layers, Appl. Mech. Rev.

Schultz, M.P., Walker, J.M. Steppe, C.N., and Flack, K.A. 2015, Impact of diatomaceous biofilms on the frictional drag of fouling-release coatings, Biofouling, vol. 31, no. 9, pp. 759–773.

Schultz, M.P. and Flack, K.A. 2005, Outer layer similarity in fully rough turbulent boundary layers, Experiments in Fluids, vol. 38, no. 3, pp. 328–340.

Sigal, A. and Danberg, J.E. 1990, New correlation of roughness density effect on the turbulent boundary layer, AIAA Journal, vol. 28, no. 3.

Simpson, R.L. 1973, A generalized correlation of roughness density effects on the turbulent boundary layer, AIAA Journal, vol. 11, no. 2, pp. 242–244.

Townsend, A. 1980, The structure of turbulent shear flow. Cambridge university press.

Song, S., Demirel, Y.K., De Marco Muscat-Fenech, D.C., Tezdogan, T., and Atlar, M. 2020, Fouling effect on the resistance of different ship types, Ocean Engineering, vol. 216, no. June, p. 107736.

van Rij, J.A., Belnap, B.J., and Ligrani, P.M. 2002, Analysis and experiments on three-dimensional, irregular surface roughness, Journal of Fluids Engineering, Transactions of the ASME, vol. 124, no. 3, pp. 671–677.

Waigh, D.R. and Kind, R.J. 1998, Improved aerodynamic characterization of regular three-dimensional roughness, AIAA Journal, vol. 36, no. 6, pp. 1117–1119.